

# In-pile CFUZ53 Sub-miniature fission chambers qualification in BR2 under PWR conditions

L. Oriol, Ch. Blandin, S. Bréaud  
CEA/DEN/Cadarache, DER/SPEX/LPE, F-13108 St. Paul-Lez-Durance, France  
loriol@cea.fr

L. Vermeeren, M. Wéber  
SCK•CEN, Nuclear Research Centre, Boeretang 200, B-2400 Mol, Belgium  
lvermeer@sckcen.be

## ABSTRACT

First prototypes of the industrial version of the CEA sub-miniature fission chambers (1.5 mm outer diameter) for in-core detection of high thermal neutron fluxes (up to  $4 \times 10^{14}$  n/(cm<sup>2</sup>.s)), manufactured by the PHOTONIS company and called CFUZ53, were tested in the CALLISTO loop of the BR2 reactor in PWR-like conditions. In this paper we present a first analysis of the recently obtained experimental results: neutron sensitivity, linearity to thermal neutron flux, current/voltage characteristics, gamma contribution, temperature effects and long term behaviour (mechanical integrity, burn-up of uranium, ...). We also compare the experimental data with calculation results from a fission chamber theoretical model. The preliminary analysis indicates that the CFUZ53 signals show consistent signals in PWR conditions up to thermal neutron fluences beyond  $2 \times 10^{20}$  n/(cm<sup>2</sup>.s).

## 1. Introduction

A new Sub-Miniature Fission Chamber (SMFC) with an outer diameter of 1.5 mm for in-core detection of high thermal neutron fluxes (up to  $4 \times 10^{14}$  n/(cm<sup>2</sup>.s)) was developed by CEA [1] and qualified in the BR2 research reactor at SCK•CEN (2001-2004) under MTR conditions (fluence up to  $3 \times 10^{21}$  n/cm<sup>2</sup>) and PWR conditions (fluence up to  $1 \times 10^{21}$  n/cm<sup>2</sup>) [2-4]. In 2004, a licence transfer of the CEA SMFC patented technology allowed the French company PHOTONIS to develop an industrial version of this fission chamber called "CFUZ53".

Three prototypes of CFUZ53 have been manufactured by PHOTONIS at the beginning of 2005 for a test irradiation in the BR2 reactor. These CFUZ53 were irradiated in the CALLISTO loop of BR2 under PWR conditions, in April-May and August 2005 (two BR2 cycles).

In this paper we will address the following aspects of the CFUZ53 behaviour: neutron sensitivity, linearity to thermal neutron flux, current/voltage characteristics, contribution of the gamma field and of the currents picked up by the sensor cable, temperature effects, long term behaviour (mechanical integrity, burn-up of uranium, ...).

We will also compare the experimental data with results from model calculations.

## 2. Description of the experiment

### 2.1 Description of the tested CFUZ53 sub-miniature fission chambers

Two CFUZ53 with a <sup>235</sup>U fissile layer of 50 µg and an argon filling gas pressure of 1.1 bar have been tested in BR2. In order to check the signal contribution due to the gamma rays and due to the current picked up by the cable, a third CFUZ53 chamber, identical to the <sup>235</sup>U sensors, but without any fissile material, was also irradiated.

The new SMFC technology is mainly characterized by the use of a special nickel and alumina gas-tight feedthrough between the chamber body and the mineral insulated cable in order to contain the filling gas on the level of the sensitive part (CEA patent [1]).

To industrialize this technology, the PHOTONIS company had to make significant efforts in order to adapt its manufacturing processes to these small dimensions (before the CFUZ53, the smallest PHOTONIS fission chambers were only 3 mm in diameter) : metal/ceramic/metal brazing of the gas-tight feedthrough, uranium deposit on the electrode with a diameter as small as 0.7 mm, assembly and TIG soldering of the different parts, void treatment and gas filling of the fission chamber.

Table 1. General technological characteristics of CFUZ53 sub-miniature fission chambers.

Nominal external diameter	1.5 mm
Sensitive length	10 mm
Electrode material	Stainless steel
Nature of fissile deposit	$^{235}\text{U}$ (93 %)
Filling gas	Argon
Coaxial cable	$\varnothing$ 1 mm ; length 20 m ; materials : stainless steel and alumina

Table 2. Specific features of the tested CFUZ53.

	FC4	FC5	FC6
Mass of $^{235}\text{U}$ ( $\mu\text{g}$ )	-	$49.5 \pm 1.3$	$50.0 \pm 1.3$
Pressure of argon (mbar)	$1100 \pm 20$	$1100 \pm 20$	$1100 \pm 20$

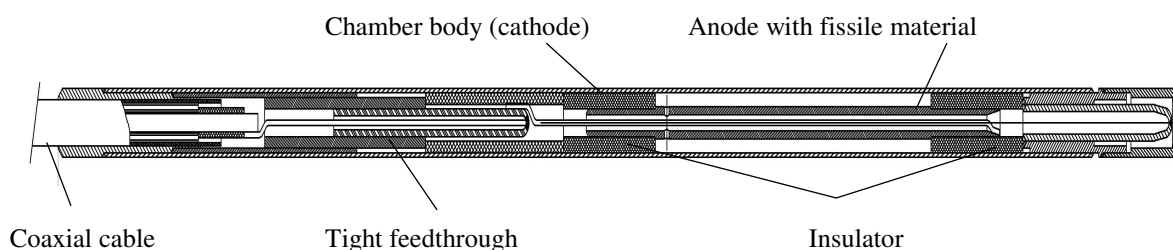


Fig. 1. Schematic view of the  $\varnothing$  1.5 mm cylindrical fission chamber (vertical scale expanded for clarity reasons)

## 2.2 Experimental conditions

The three CFUZ53 were mounted on an experimental device which was also equipped with a rhodium self-powered neutron detector (SPND), a gamma thermometer and a thermocouple. The device was introduced in one of the three legs (IPS, in-pile sections) of the CALLISTO loop in the BR2 reactor (channel K311) and irradiated during two BR2 reactor cycles (i.e. about 1000 h). The thermal neutron flux and gamma heating were monitored on-line by means of the Rh-SPND and the gamma thermometer, respectively. An independent verification of the neutron flux data (thermal, epithermal and fast) will be accomplished using the time-integrated data from activation dosimetry with AlCo, AlAg and Ni samples.

The CALLISTO loop was operated at the following thermohydraulic conditions : inlet temperature of 260°C to 300°C, coolant pressure of 15.5 MPa, flow rate in the IPS of 1.3 kg/s.

The chemical composition of the CALLISTO cooling water represents that of a PWR primary circuit. Typical conditions are (allowing some variations) : boron (boric acid):  $\pm 550$  ppm, lithium (lithium hydroxide):  $1.7 \text{ ppm} \leq [\text{Li}] \leq 2.4 \text{ ppm}$ , pH:  $6.78 \leq \text{pH}_{25^\circ\text{C}} \leq 6.95$  or  $7.13 \leq \text{pH}_{300^\circ\text{C}} \leq 7.27$ , dissolved hydrogen:  $25 \text{ ccSTP/kg} \leq [\text{H}_2] \leq 35 \text{ ccSTP/kg}$ .

At the nominal reactor power of 56 MW and at a temperature of 290°C, the SPND signals yielded values for the conventional thermal neutron flux  $n_{v_0}$  (Stoughton-Halperin convention [5]) of  $6 \times 10^{13} \text{ n}/(\text{cm}^2 \cdot \text{s})$ , which corresponds to a “real” thermal flux (integrated up to 0.5 eV) [5] of  $1.1 \times 10^{14} \text{ n}/(\text{cm}^2 \cdot \text{s})$ . The epithermal and fast fluxes will be assessed later; predicted values based on core calculations are  $6 \times 10^{12} \text{ n}/(\text{cm}^2 \cdot \text{s})$  per unit lethargy for the epithermal flux and  $5 \times 10^{13} \text{ n}/(\text{cm}^2 \cdot \text{s})$  for the fast flux ( $E > 0.1 \text{ MeV}$ ). The measured value of the gamma heating rate was 1.2 W/g (predicted value: 1.0 W/g).

### 3. Experimental results

#### 3.1 Chamber without fissile deposit

The total current of the chamber without fissile deposit (FC4) can be considered as the sum of two contributions : (i) the current  $I_c$  induced in the cable, (ii) the current  $I_\gamma$  due to gamma-induced ionization of the filling gas in the sensitive zone. The cable-induced current  $I_c$  is mainly due to the radiation-induced drop in the cable insulation resistance and is thus proportional to the applied voltage, whereas the  $I_\gamma$  dependence on the voltage shows a normal ionization chamber behaviour with a more or less constant value over a broad voltage range (saturation plateau). This is illustrated in Fig. 2, which shows the recorded current/voltage profiles (normalized to nominal reactor power) for various BR2 power levels. The normalized data can be interpreted in terms of a  $I_\gamma$  contribution of about 2.0  $\mu\text{A}$  (the zero intercept of all extrapolated curves) and a  $I_c$  contribution proportional to the polarization voltage ranging from about 25 nA/V (at low power) to 8.5 nA/V (at high power). The constant (normalized) value of  $I_\gamma$  implies that the gamma contribution to the signal scales perfectly with the reactor power. From the  $I_c$  data effective isolation resistance values can be determined ranging from 4 G $\Omega$  (at 1% reactor power) to 0.13 G $\Omega$  (at 90% reactor power).  $I_\gamma$  and  $I_c$  turn out to be of the same order,  $I_\gamma$  being dominant at polarization voltages below 100 V and  $I_c$  at higher voltages.

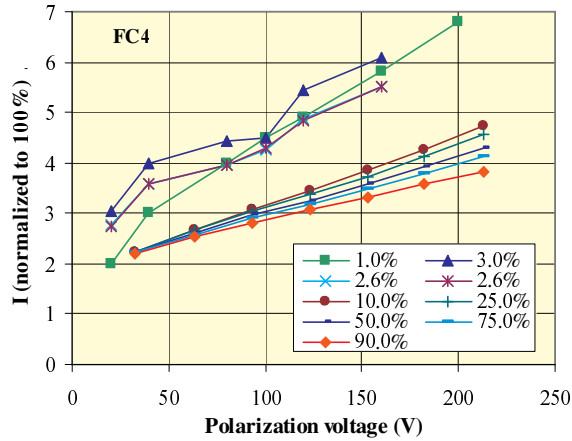


Fig. 2.  $I/V$  curves for the fission chamber without fissile layer at various reactor power values. The data are expressed in  $\mu\text{A}$ , normalized to 100% reactor power (56 MW)

#### 3.2 Saturation curves

The CFUZ53 currents were recorded as a function of the applied voltage (saturation curves) for various neutron fluxes during the stepwise startup of the reactor. Figure 3 shows the recorded data for the two fission chambers with fissile deposit (FC5 and FC6) for reactor power values between 10 and 90%.

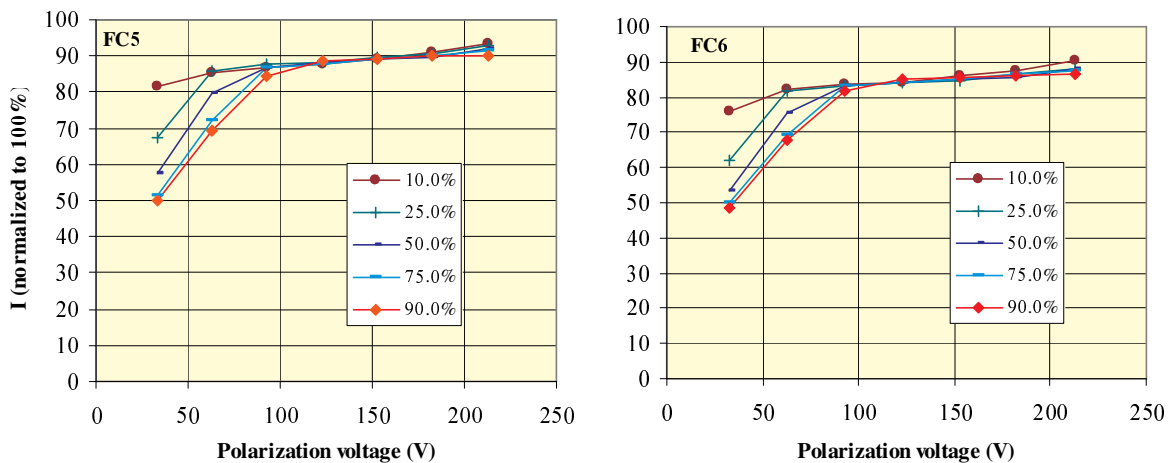


Fig. 3.  $I/V$  curves for FC5 and FC6 at various reactor power values. The data are expressed in  $\mu\text{A}$ , normalized to 100% reactor power (56 MW).

The datasets for both detectors are very similar. The neutron flux dependence of the threshold polarization voltage needed for a complete collection of all charge is clearly visible. In the middle of the saturation plateau, all curves coincide, indicating the proportionality of the fission chamber signal with the reactor power. A 140 V polarization voltage was chosen for the continuous neutron flux measurements.

### 3.3 Linearity of the response versus the neutron flux

Figure 4 illustrates the linearity of the fission chamber response (corrected for gamma and cable contributions by subtraction of the FC4 signal) as a function of the thermal neutron flux during restart of the BR2 reactor. Following the Stoughton-Halperin convention as discussed in [5], the thermal flux was defined as  $\Phi_{th,conv} = n_{th} \cdot v_o$ , in which  $n_{th}$  is the purely thermal part of the neutron density and  $v_o$  the most probable neutron velocity at  $T_o = 293.4$  K (2200 m/s). At the relatively high irradiation temperatures, the “true” thermal neutron flux taking into account the real velocity of every thermal neutron [5] is significantly higher.

The local thermal neutron flux at the fission chambers position was monitored by the signal of a Rh SPND located nearby. From full-core MCNP calculations the flux gradients between the different sensors were assessed. Deviations were found to be smaller than  $\pm 1\%$ , so they will be neglected in this analysis. The conversion of the SPND currents to thermal flux values was based on an initial detector sensitivity of  $1.447 \times 10^{-20}$  A/(n/cm<sup>2</sup>s), obtained by convoluting the calculated local neutron spectrum with the energy-dependent sensitivity calculated separately using a MCNP-based SPND model [6]. A correction was also made for the reduced sensitivity due to Rh depletion in the SPND emitter (1.5% reduction at a thermal neutron fluence of  $1.15 \times 10^{20}$  n/cm<sup>2</sup> accumulated at the moment the data of figure 6 were taken).

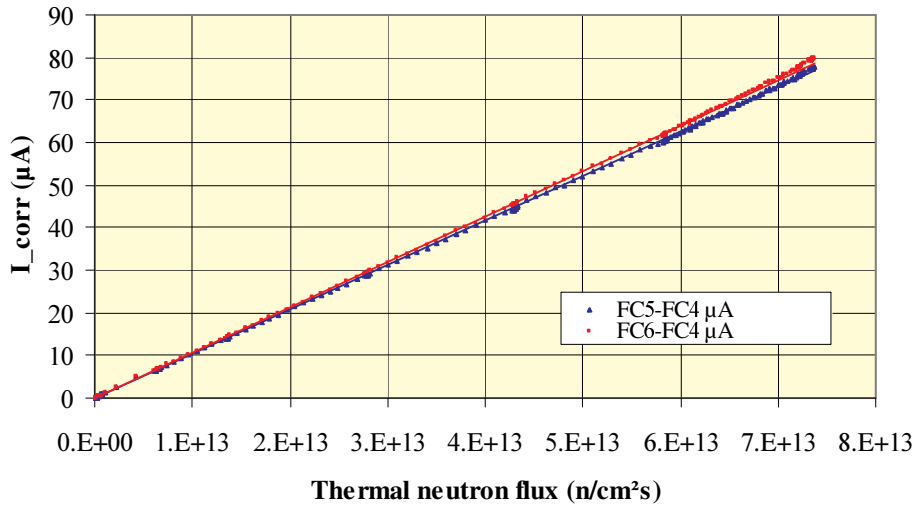


Fig. 4: Thermal neutron flux dependence of CFUZ53 currents ( $V_{pol} = 140$  V) corrected for  $I_\gamma$  and  $I_c$  contributions ( $I_{FC5} - I_{FC4}$  and  $I_{FC6} - I_{FC4}$ ), measured during reactor restart after an accumulated thermal neutron fluence of  $1.15 \times 10^{20}$  n/cm<sup>2</sup>. The thermal neutron flux data were obtained from the SPND signals.

### 3.4 Sensitivity of fission chambers

In view of the good linearity of the fission chambers response (including a very small zero intercept) the experimental thermal neutron sensitivities (net current per thermal neutron flux unit) is defined by the following formula :

$$S_{exp.5,6} = \frac{I_{FC5,FC6} - I_{FC4}}{\phi_{th,conv}(I_{SPND})} \quad (1)$$

where  $I_{FCn}$  are the currents delivered by the FC and  $\phi_{th,conv}(I_{SPND})$  is the conventional thermal flux deduced from the SPND current as described in the previous section.

As it will be seen later, this sensitivity depends on the depletion (burnup) of the fissile deposit with the neutron fluence. It can also show some slight variations with modifications of the neutron spectrum due to changes in the core configuration (see section 3.5).

### 3.5 Long term performance

The long term performance of the CFUZ53 was investigated, for a first step (see section 5 for future long term experimentation), up to a neutron fluence of  $2.3 \times 10^{20}$  n/cm<sup>2</sup> which is the order of magnitude of the fluence corresponding to one cycle in a PWR. The current-voltage profiles remain unaffected (observation of correct saturation domains, which even shift to lower voltages as the currents are dropping).

The sensitivity (as defined by equation (1)) was continuously monitored. Due to the gradual consumption of the <sup>235</sup>U deposit, it is expected to drop exponentially as a function of the thermal neutron fluence  $\phi t$  :

$$S(\phi t) = S(\phi t = 0) \cdot \exp(-\sigma_a \phi t) \quad (2)$$

Assuming an epithermal index of 0.05, the thermal neutron absorption (fission plus capture) cross section of 680 b [7] and the corresponding resonance integral of 419 b [7] lead to an effective neutron absorption cross section  $\sigma_a = 700$  b. This results in a sensitivity at the final fluence of 85% of the initial value.

Figure 5 shows the long term evolution of the fission chamber sensitivity, corrected for the expected sensitivity loss discussed above. After a rather fast initial sensitivity drop, the data are fluctuating around an equilibrium value, so the sensitivity evolution is quite well described by equation (2). Some of the deviations from the average value can be related to reactor configuration changes (see figure 6): the loading/unloading of uranium targets in a neighbouring reactor channel. Also the start of the new reactor cycle (with a slightly different configuration) causes a change in the measured sensitivity. At each of these configuration changes, the gradient between the SPND and fission chambers might be influenced and also the neutron spectrum at the detectors' location is affected. Both aspects will cause a change in the ratio between the fission chamber and the SPND response (both types of detectors have a slightly different spectral response) and so the sensitivity values calculated from (1) are influenced.

The initial fast sensitivity had already been observed before when irradiating prototype fission chambers with similar design. It was explained by a degradation of the filling gas due to outgassing of the walls (mainly the anode with uranium deposit) at the irradiation temperature of about 300°C. As the CFUZ53 fission chambers were carefully outgassed during the manufacturing process, the reason for the similar behaviour for these detectors is still under analysis.

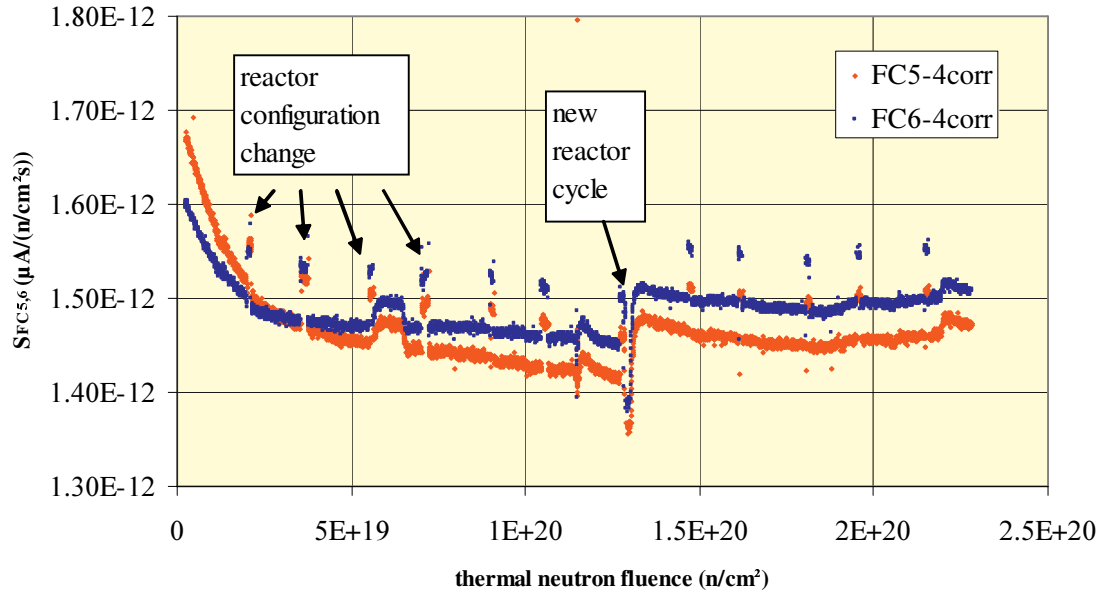


Figure 5: Long term evolution of the CFUZ53 sensitivities calculated according to equation (1), corrected for the expected sensitivity drop due to uranium consumption. The arrows indicate identified correlations between apparent sensitivity changes and changes in reactor configuration (loading/unloading of uranium targets in neighbouring channel and start of new reactor cycle).

### 3.6 Temperature effect

Although during most of the irradiation the temperature was kept between 290 and 295°C, some tests were performed at lower temperatures (down to 265°C). Figure 6 shows the relative CFUZ53 and SPND data recorded while changing the temperature (all other conditions remaining essentially constant). At 270°C, the CFUZ53 signals are about 2% higher than at 290°C; for the SPND the temperature dependence is smaller, about 0.7% difference between 270°C and 290°C. The temperature dependence can be explained by the fact that the conventional thermal neutron flux, as defined in 3.3, decreases with increasing temperature. Considering only the purely thermal part, the conventional neutron flux is proportional to the inverse of the square root of the absolute temperature, which is in fact due to the increased average neutron energy combined with an ideal  $1/v$  cross section dependence. This proportionality would lead to a relative flux difference between 270°C and 290°C of 1.8%, which is consistent with the CFUZ53 signal change. The Rh SPND signal depends less with temperature, because the rhodium neutron capture cross section deviates more from a  $1/v$  shape, having a strong resonance around 1 eV.

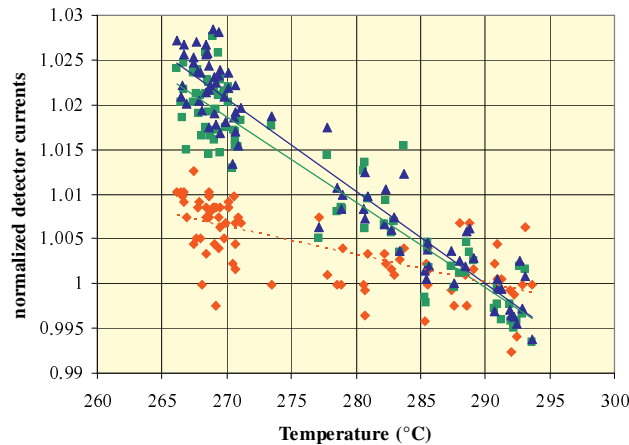


Figure 6: Temperature dependence of the CFUZ53 (FC5, green squares, and FC6, blue triangles) and SPND (red diamonds, dotted line) signals, normalized to the 290°C value.

#### 4. Theoretical Model

The FCD (Fission Chamber Designer) computer code, conceived especially for chambers operating in a current mode, is based on a theoretical model which includes the electric field distortion resulting from the charge collection effect [8]. FCD calculates the neutron sensitivity and the limits of the CFUZ53 saturation domain, with the applied voltage and the  $^{235}\text{U}$  fission rate as parameters. Fig. 7 shows the calculated correlation between the lower voltage limits of the saturation domain and the CFUZ53 current; the experimental data are well described. For the neutron sensitivity calculation, the procedure described in the reference quoted above adopts the asymptotic hypothesis  $r_a \gg (r_c - r_a)$ , with  $r_c$  and  $r_a$  the cathode and the anode radius, which is not fulfilled in our case.

A more general treatment, which only assumes isotropic emission of the fission fragments and straight fission fragment paths with a constant energy loss per unit length, leads to the following expression for the sensitivity  $S$  :

$$S = 2\pi e L I_o p N_A \frac{\mu_s}{M} \sigma_{eff} r_a r_c \left[ E\left(\frac{r_a}{r_c}\right) - \frac{r_a}{r_c} \right] \quad (3)$$

where :  $I_o$  = number of ion-pairs created per fission fragment per unit length per unit pressure,  $L$  = sensitive length,  $p$  = argon pressure,  $\mu_s$  = surfacic mass of  $^{235}\text{U}$ ,  $M$  = molar mass,  $N_a$  = Avogadro number,  $\sigma_{eff}$  = fission cross section = 596 b (assuming an epithermal index of 0.05), and  $E(k)$  the elliptic

integral of the second kind :  $E(k) = \int_0^{\pi/2} \sqrt{1 - k^2 \sin^2 x} dx$ .

For the studied CFUZ53 version ( $50 \mu\text{g } ^{235}\text{U}$ ), this leads to a theoretical initial sensitivity of  $1.58 \times 10^{-18} \text{ A}/(\text{n}/\text{cm}^2\text{s})$ , which is in good agreement with the observed data (see Fig. 5).

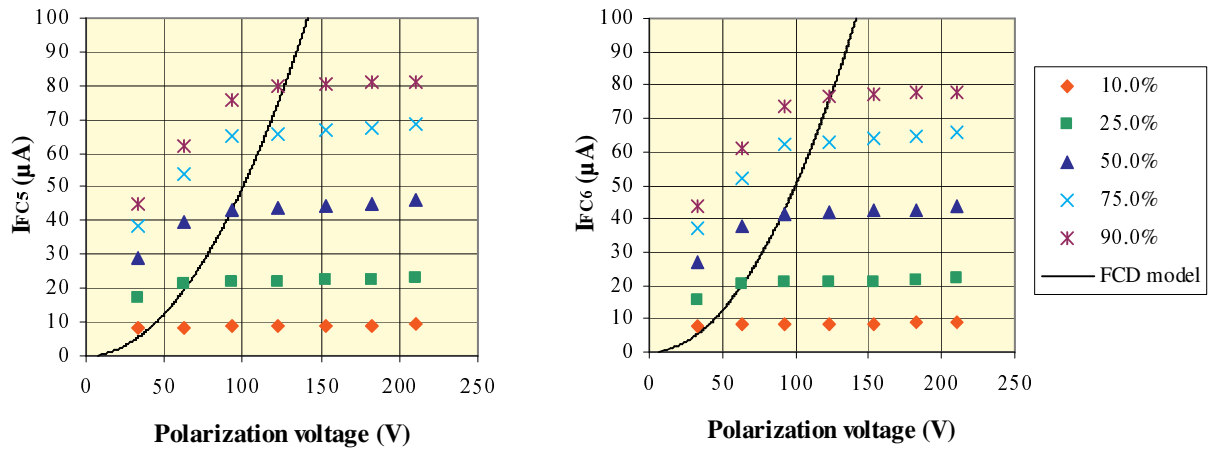


Fig. 7. Experimental saturation curves of FC5 and FC6 in BR2 for thermal neutron fluxes ranging from  $7 \times 10^{12} \text{ n}/(\text{cm}^2\text{s})$  to  $6.3 \times 10^{13} \text{ n}/(\text{cm}^2\text{s})$ . The theoretical onsets of the saturation domain (obtained from the FCD code) are represented by the full curves.

## 5. Conclusions and perspectives

After this significant experimental campaign in the CALLISTO loop of the BR2 reactor in PWR conditions, we are very confident in the PHOTONIS CFUZ53 fission chamber which is the industrialized version of the uranium 1.5 mm sub-miniature fission chamber developed by the CEA.

This detector will be further qualified in the CALLISTO loop in higher and faster fluxes during a long term campaign of 10 BR2 irradiation cycles beginning in April 2006 (about 5 000 hours corresponding to a predicted fluence of about  $2 \times 10^{21}$  n/(cm<sup>2</sup> s) equivalent to 4 cycles in a PWR).

A new type of sub-miniature fission chamber is being developed by the CEA in collaboration with PHOTONIS. This detector called CFPZ aimed at measuring fast neutron fluxes (> 1 MeV) will have a <sup>242</sup>Pu fissile coating and will be connected to a new 50 Ω cable that will allow pulse and Campbelling mode measurements. This type of detector will require a specific large dynamics electronics supporting the three modes (pulse/Campbelling/current) which is also under development at the CEA [9].

First tests of the CEA prototype of the CFPZ fast flux sub-miniature fission chamber are planned for the end of 2005 at the French OSIRIS reactor. More complete and long term tests will be performed in the BR2 reactor from mid 2006.

## 6. References

- [1] G. Bignan and J.C. Guyard, *Sub-miniature fission chamber with tight feedthrough*, Patent CEA N° 94-14293 (1994)
- [2] Ch. Blandin, S. Breaud, L. Vermeeren and M. Wéber, *Development of new sub-miniature fission chambers: modeling and experimental tests*, Proc. SMORN-VIII Symposium, Göteborg, Sweden, May 27-31, 2002.
- [3] L. Vermeeren, M. Wéber, Ch. Blandin and S. Breaud, *In-pile sub-miniature fission chambers testing in BR2*, Proc. 11<sup>th</sup> Int. Symp. on Reactor Dosimetry, Brussels, Aug. 18-23, 2002, eds. J. Wagemans et al., World Scientific, 2003, pp.364-371.
- [4] M. Wéber, R.-W. Bosch and L. Vermeeren, *Design and development of a multipurpose PWR rig for in-core instrumented testing*, Proc. Int. Conf. Water Chemistry of Nuclear Reactor Systems, San Francisco, USA, October 2004.
- [5] ASTM Standard E262-86, *Standard test method for determining thermal neutron reaction and fluence rates by radioactivation techniques* (1991).
- [6] L. Vermeeren and M. Wéber, *Self-powered neutron detector qualification for absolute on-line in-pile neutron flux measurements in BR2*, Proc. 11<sup>th</sup> Int. Symp. on Reactor Dosimetry, Brussels, Aug. 18-23, 2002, eds. J. Wagemans et al., World Scientific, 2003, pp.219-225.
- [7] S.F. Mughabghab, *Neutron cross sections, Neutron resonance parameters and thermal cross sections*, vol. 1, NNDC-BNL (1984).
- [8] O. Poujade and A. Lebrun, *Modeling of the Saturation Current of a Fission Chamber taking into Account the Distortion of Electric Field due to Space Charge Effects*, Nuclear Instruments and Methods in Physics Research A443 (1999) 673-682.
- [9] S. Normand, *A new system for in-core wide range neutron monitoring*, IEEE Nuclear Science Symposium, Roma, 2004.